Second harmonic generation as a probe of parametric spin wave instability processes in thin magnetic films

P. N. Solovev,[1,*] A. O. Afonin,[1] B. A. Belyaev,[1,2] N. M. Boev,[1,2] I. V. Govorun,[1] A. V. Izotov,[1,2] A. V. Ugrymov,[1] and A. A. Leksikov[1]

[1]*Kirensky Institute of Physics, Federal Research Center KSC SB RAS, 660036, Krasnoyarsk, Russia*

[2]*Institute of Engineering Physics and Radio Electronics, Siberian Federal University, 660041, Krasnoyarsk, Russia*

(Received 30 April 2022; accepted 19 July 2022; published 3 August 2022)

We have explored the dynamic response of in-plane magnetized thin permalloy films excited by microwave fields of high amplitudes (up to 3 Oe) at 1 GHz. The response was detected using a microstrip line by measuring the second harmonic signal generated by the dynamic components of the uniform magnetization. The data measured at ferromagnetic resonance showed the threshold effect of the Suhl parametric instability process. With the increase of the microwave power above the threshold value, the dynamic response revealed an intricate nonlinear behavior, including the emergence of an additional threshold. This second threshold can be explained in terms of the "stage by stage" process of parametric spin wave excitation following the *S* theory of Zakharov, L'vov, and Starobinets.

DOI: 10.1103/PhysRevB.106.064406

I. INTRODUCTION

Depending on the amplitude of the microwave driving field, the high-frequency behavior of a magnetic material exhibits linear or nonlinear properties. At low microwave power levels, the dynamics of the magnetization can be approximately described by the linearized equation of motion [1]. In this regime, the components of the dynamic magnetization depend linearly on the microwave field amplitude. However, since magnetization dynamics is inherently nonlinear, at higher microwave powers and larger amplitudes of the uniform magnetization precession, the linear relationship between the magnetization and the microwave field is disrupted, and the magnetic system displays a rich set of nonlinear effects [2,3].

A prominent example of such nonlinear phenomena that occur in magnetic materials is the premature saturation effect of the ferromagnetic resonance (FMR). This effect was first observed more than half a century ago in ferrites [4] and was explained by Suhl in terms of parametric resonance in a continuous medium [5–7]. According to the Suhl theory, when the microwave power is above a certain threshold level, the uniform precession mode can parametrically excite a pair of degenerate spin waves. During this instability process, the parametric spin waves gain energy from the uniform mode, which results in the decrease of the effective susceptibility at high-power FMR. Later it was also shown that parametric spin waves with half the frequency of the driving field could be excited directly by the microwave field applied parallel to the equilibrium magnetization direction [8]. Since then, these nonlinear processes have been extensively studied in the context of understanding the fundamental physics and for technological applications as well [1,2,9].

Traditionally, high-power microwave experiments were carried out using ferrites, owing to their unique properties, most importantly, extremely low magnetic damping. However, from the point of view of modern technical applications, ferrites have several drawbacks. These include low saturation magnetization limiting their operating frequency band, relatively low Curie point, and compatibility issues with conventional semiconductor technology. Therefore, in recent years the focus of research has shifted toward thin metallic magnetic films, particularly those made of permalloy ($Ni_{80}Fe_{20}$). In contrast to ferrites, such films can be readily integrated with complementary metal oxide semiconductor (CMOS) processes, they have relatively high saturation magnetization and high-frequency susceptibility. In the last 15 years, there has been an upsurge of interest in parametric processes in thin metallic films and nanostructures [10–16], raised by the importance of these nonlinear effects in the large-angle magnetization switching [17], which is relevant, for example, in magnetic memory devices and spin-torque nano-oscillators [18]. Moreover, a detailed understanding of the parametric instability processes is an essential step on the way to next-generation nonlinear microwave signal processing devices based on thin magnetic films and thin-film nanostructures [19,20].

In this paper, we report an investigation of the nonlinear microwave behavior of thin permalloy films by measuring the second harmonic generation. The sample was placed inside the microstrip line, where the signal line served simultaneously as an emitter of a microwave driving field and as an antenna that receives the second harmonic signal generated by the film. At ferromagnetic resonance, the main source of this signal is the longitudinal time-dependent component of the uniform magnetization, which oscillates at twice the

*psolovev@iph.krasn.ru

 ©2022 American Physical Society

frequency of the driving field and emerges due to the highly elliptic precession orbit [21]. Unlike the absorption technique that is widely employed in high-power FMR experiments (e.g., vector network analyzer FMR [13,14]), the method of inductive detection of the second harmonic signal used in this work allows for the direct quantitative measurements of the uniform magnetization precession amplitude. These measurements of the second harmonic generation versus input power show a clear signature of the second-order parametric processes. Surprisingly, in addition to the expected power threshold at a relatively low microwave field, the measurements also reveal the appearance of the second threshold at a much higher microwave field. These findings are discussed in the framework of the Suhl parametric instability theory and the S theory [22], which takes into account the interactions of parametric spin waves.

II. THIN-FILM SAMPLE, ITS CHARACTERIZATION, AND SECOND HARMONIC MEASUREMENTS SETUP

The studied nanocrystalline thin magnetic film with a thickness of 100 nm was produced by DC magnetron sputtering of a $Ni_{80}Fe_{20}$ target on a heated to 200 °C quartz glass substrate, $3\times5\times0.5\,\mathrm{mm}^3$ in size. The base pressure was 2.2×10^{-6} Torr, and the argon pressure was 1.5×10^{-3} Torr. Prior to the magnetic film deposition, a 200 nm thick SiO layer was thermally deposited on the substrate to improve the homogeneity of the magnetic film. During the sputtering, a uniform in-plane static magnetic field of ~200 Oe was applied to the film along its long side to induce a uniaxial magnetic anisotropy.

The magnetic properties of the produced sample were determined using a scanning FMR spectrometer [23]. The absorption spectra were measured from local areas on the surface of the film (~0.8 mm in diameter) at a fixed pumping frequency of $f = 2.5$ GHz while sweeping the in-plane magnetic field. From the angular dependences of the resonance field, using a special fitting procedure based on a single domain model of a magnetic film [24], we determined the effective saturation magnetization M_{eff}, the uniaxial anisotropy field H_u, and the easy axis direction θ_u. Also, from the measured spectra, we obtained the FMR linewidth ΔH. The parameters averaged over the film surface were the following: $M_{\mathrm{eff}} = 872\,\mathrm{emu/cm}^3$, $H_u = 3$ Oe, $\theta_u = -0.5°$, $\Delta H = 18$ Oe, and the corresponding Gilbert damping parameter $\alpha = \gamma\Delta H/(4\pi f)$ is 0.01 ($\gamma = 1.76\times10^7$ rad/sOe is the gyromagnetic ratio). The distributions of these magnetic parameters across the film surface are shown in the Supplemental Material [25]. Note that the determined effective magnetization is $M_{\mathrm{eff}} = M_s – H_p/4\pi$, where M_s is the saturation magnetization and H_p is the field of the magnetic anisotropy perpendicular to the film plane [24]. However, in nanocrystalline permalloy films $H_p \ll 4\pi M_s$, and it can be considered approximately that $M_{\mathrm{eff}} \approx M_s$.

Figure 1(a) shows schematically the experimental setup used for the measurements of the second harmonic generation in a thin magnetic film as a function of the static and microwave magnetic fields. The in-plane static magnetic field was produced by Helmholtz coils which were placed on a platform rotated by a stepper motor. A microstrip line was

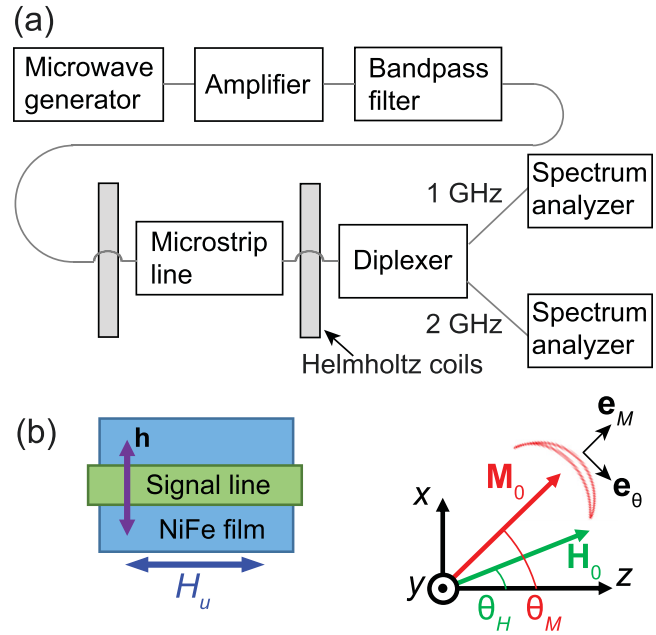

FIG. 1. (a) The schematic representation of the experimental setup used for the second harmonic measurements. (b) The sketch of the sample under the signal line and the coordinate system, where $\mathbf{M}_0$ is the equilibrium magnetization, $\mathbf{H_0}$ is the external static magnetic field, H_u is the uniaxial anisotropy field, and $\mathbf{h}$ is the microwave driving field. $\mathbf{e}_\theta$ and $\mathbf{e}_M$ are the unit vectors that define the coordinate system related to the equilibrium magnetization $\mathbf{M}_0$.

used to transmit and receive a microwave signal to and from the film. The signal line made of Cu had a thickness of 17 μm, length of 5 mm, and width $w = 1$ mm. The sample was inserted between the signal line and a ground plane, with the magnetic film facing the signal line. The microstrip line was adjusted to have the characteristic impedance $Z_0 = 50\Omega$. The input signal at a frequency of 1 GHz provided by a microwave generator and amplified by a power amplifier was sent through a filter with a bandpass at a frequency of 1 GHz [26] so that any higher-harmonic components were eliminated from the amplified signal before entering the film. A diplexer [27] connected to the output of the transmission line split the output signal into two channels, at 1 and 2 GHz. The signals from each channel were received by the spectrum analyzers, thus allowing us to simultaneously measure the power of the second harmonic generated by the film at 2 GHz and the power absorbed by the film at 1 GHz. The power losses were measured for all cables and interconnections to determine the true microwave power received and transmitted by the microstrip line.

However, if we want to directly compare the experimental and theoretical results, we have to convert the input and output powers to a field and a magnetization. The amplitude of the driving microwave field h produced by the microstrip line can be estimated as $h = 4\pi\,10^{-3}(P_1/4Z_0w^2)^{1/2}$ (expressed in Oe), where P_1 is the power of the input signal [28]. The second harmonic signal comes from the second-order dynamic magnetization component m_{2x} (as will be discussed later) that oscillates at twice the frequency of the input signal. The magnetic flux from this component winds around the signal

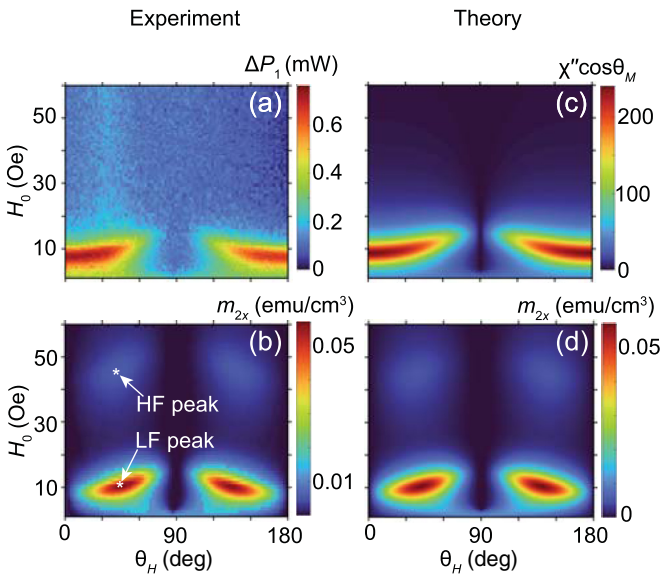

FIG. 2. The dependencies of the FMR absorption (at 1 GHz) (a,c) and second harmonic generation (at 2 GHz) (b,d) in a 100 nm thick $Ni_{80}Fe_{20}$ film on the direction θ_H and strength H_0 of the applied static magnetic field. (a,b) are experimental results and (c,d) theoretical ones. The input signal power at a frequency of 1 GHz was 10 mW (the microwave field amplitude $h = 0.09$ Oe). ΔP_1 is the power absorbed at 1 GHz, which is proportional to the imaginary part of the magnetic permeability χ'', and m_{2x} is the amplitude of the second-order dynamic magnetization, which is the source of the second harmonic signal at 2 GHz (see text for details).

line, and, through Faraday's law, we can relate the amplitude m_{2x} to the detected power P_2 of the second harmonic signal as [28,29]

$$m_{2x} = \frac{2\sqrt{2P_2Z_0}}{10^3 d_m \omega_2 \mu_0 l t_F}, \tag{1}$$

where l and t_F are the length and thickness of the magnetic film, μ_0 is the magnetic constant, ω_2 is the circular frequency of m_{2x} oscillation, and d_m is the coefficient that accounts for losses of various types; for our case we estimated it to be 0.89. Note that the value of m_{2x}, according to Eq. (1), is expressed in emu/cm^3 (see [29]).

III. SECOND HARMONIC GENERATION AT LOW MICROWAVE SIGNAL POWER

A. Experiment

We start our study by first considering the case of a low-power input signal. Figures 2(a) and 2(b) show the result of measuring simultaneously the power absorption and generated second harmonic amplitude as a function of the direction θ_H and the strength H_0 of the static magnetic field produced by the Helmholtz coils. The input signal power at a frequency of $f_1 = 1$ GHz was $P_1 = 10$ mW, corresponding to the microwave field amplitude $h = 0.09$ Oe. The map [Fig. 2(a)] of the absorbed power ΔP_1 at 1 GHz demonstrates the usual FMR response of a magnetic film, where the peaks of ΔP_1 form the well-known angular dependence of the resonance field. As the angle of the static field θ_H increases from 0° to 90°, the equilibrium magnetization $\mathbf{M}_0$ rotates toward the microwave field $\mathbf{h}$ [Fig. 1(b)] resulting in the weakening of the interaction between $\mathbf{M}_0$ and $\mathbf{h}$, until at $\theta_H = 90°$ (when $\mathbf{M}_0 \| \mathbf{h}$) there is no absorption at all.

Figure 2(b) presents the map of the second-order magnetization m_{2x}, which was obtained from the measured output power P_2 at 2 GHz using Eq. (1). The mirror symmetry observed along the θ_H axis is due to the uniaxial magnetic anisotropy of the film [Fig. 1(b)]. At the same time, as one can see, m_{2x} has two local maxima along the field axis H_0: The first one is at the field $H_0 = 10.6$ Oe and $\theta_H = 45°$, which can be denoted as the low-field (LF) peak, and the second one is at $H_0 = 46.5$ Oe and $\theta_H = 43°$—the high-field (HF) peak. The amplitude of the LF peak is an order of magnitude larger than the amplitude of the HF peak.

B. Second-order perturbation theory

This interesting behavior of the second-order magnetization was theoretically analyzed in detail in our previous paper [29], in the approximation of the low driving field amplitude. Here we present a summary of the obtained results. The Landau-Lifshitz-Gilbert (LLG) equation describes the dynamics of the magnetization $\mathbf{M}$ in a ferromagnet [1]. This differential equation is nonlinear, but in the case of small magnetization precession angles, the approximate analytical solution can be found using a perturbation approach. To obtain the expressions for the uniform magnetization component oscillating at a double frequency of the driving field, we expand the magnetization $\mathbf{M}$ to the second-order term and seek the solution of the LLG equation in the form $\mathbf{M} = \mathbf{M}_0 + \mathbf{m}_1(t) + \mathbf{m}_2(t)$, where $m_2 \ll m_1 \ll M_0$. First, retaining only terms of the first order of smallness, the solution for the first-order dynamic component $\mathbf{m}_1$ that has a frequency of the driving field is found, and then this solution is substituted in the initial equation to find the second-order component $\mathbf{m}_2$, oscillating at twice the frequency of the driving field [29].

The amplitude of the main component of the first-order magnetization can be expressed as $m_{1\theta} = |\chi| h_\theta$, where χ is the magnetic susceptibility, and h_θ is the transverse [with respect to the equilibrium magnetization $\mathbf{M}_0$; see Fig. 1(b)] component of the driving field. For a thin film with uniaxial anisotropy, the susceptibility χ is given by

$$\chi = \frac{1}{4\pi} \frac{\omega_M \omega_y}{\omega_0^2 - \omega^2 + i\alpha\omega(\omega_y + \omega_\theta)}, \tag{2}$$

where $\omega = 2\pi f$ is the circular frequency of the driving field, $\omega_M = 4\pi\gamma M_s$, and $\omega_0 = 2\pi f_0 = \sqrt{\omega_\theta \omega_y}$ is the FMR frequency. The parameters ω_y and ω_θ are

$$\begin{aligned} \omega_y &= \gamma[H_0 \cos(\theta_H - \theta_M) + H_u \cos^2\theta_M + 4\pi M_s], \\ \omega_\theta &= \gamma[H_0 \cos(\theta_H - \theta_M) + H_u \cos 2\theta_M], \end{aligned} \tag{3}$$

where θ_M is the angle of the orientation of the equilibrium magnetization $\mathbf{M}_0$.

The second-order magnetization $\mathbf{m}_2$ consists of two main contributing components, the transverse $m_{2\theta}$, and the longitudinal m_{2M}. The longitudinal component m_{2M} is associated with the ellipticity of the magnetization vector precession in the $(\mathbf{e}_\theta, \mathbf{e}_y)$ plane and the conservation of the magnetization vector length. Its amplitude can be approximately

expressed as

$$m_{2M} = (1/4M_s)m_{1\theta}^2 = (1/4M_s)|\chi^2|h_\theta^2. \quad (4)$$

This component gives the largest contribution to $\mathbf{m}_2$ and reaches a maximum at the same conditions as $m_{1\theta}$, that is, at FMR. The m_{2M} is responsible for the LF peak in the second harmonic generation observed in the experiment.

The transverse second-order component $m_{2\theta}$ emerges due to the modulation of the magnetization precession by the longitudinal component of the driving field h_M. The amplitude of $m_{2\theta}$ can be written as

$$m_{2\theta} = |(1/D_2)C\chi|h_\theta h_M, \quad (5)$$

where $D_2 = \omega_0 – 4\omega^2 + i\alpha 2\omega(\omega_y + \omega_\theta)$, and $C = \gamma(\omega_y + i\alpha 2\omega)/2$. The important feature of $m_{2\theta}$ is that it has two peaks. The first one, associated with the χ term, is at FMR. The second peak follows from the resonancelike behavior of the denominator D_2, which is minimum at half the frequency of the FMR or, in the case of the fixed driving frequency, in the corresponding higher magnetic field. This second peak of $m_{2\theta}$ explains the HF peak observed in the experiment. Considering the geometry of the measurements, the resulting second harmonic output signal is determined as

$$m_{2x} = m_{2M}\sin\theta_M + m_{2\theta}\cos\theta_M. \quad (6)$$

Figures 2(c) and 2(d) display the theoretical results obtained using expressions presented above for the parameters of the experimental sample. Because the imaginary part of susceptibility χ'' is proportional to the microwave power absorbed by the film, in Fig. 2(c), we have plotted the dependence of $\chi''\cos\theta_M$ on H_0 and θ_H, calculated using Eq. (2) for $f = f_1 = 1$ GHz. As expected, there is good agreement with the experimental dependency of $\Delta P_1(H_0, \theta_H)$ shown in Fig. 2(a). For the same parameters, Fig. 2(d) shows the map of the second-order magnetization m_{2x} calculated with Eq. (6). A good accordance between theory and experiment can be observed here also, where not only the positions of the LF and HF peaks but also their amplitudes and linewidths agree well with the experiment [Fig. 2(b)]. We conclude that the solution obtained in the frame of a perturbation approach for the uniform magnetization precession describes accurately the dynamic behavior of the first- and second-order magnetizations in the case of a low-amplitude microwave field.

IV. SECOND HARMONIC GENERATION AT HIGH MICROWAVE SIGNAL POWERS

A. Experiment

For the same frequency of the input signal (1 GHz), we have investigated the behavior of the second harmonic amplitude as a function of the microwave field amplitude h. The maximum power of the input signal was 10 W, which corresponds to $h = 2.8$ Oe. Figure 3 shows the maps $m_{2x}(H_0, \theta_H)$, which are analogous to those in Fig. 2 but obtained at higher signal powers. As one can see, the increase in the microwave field amplitude leads to the change in the LF peak shape, which becomes more "round," and also to its shift to the lower values of the field H_0. The HF peak shape and position, however, do not change much but the peak appears brighter,

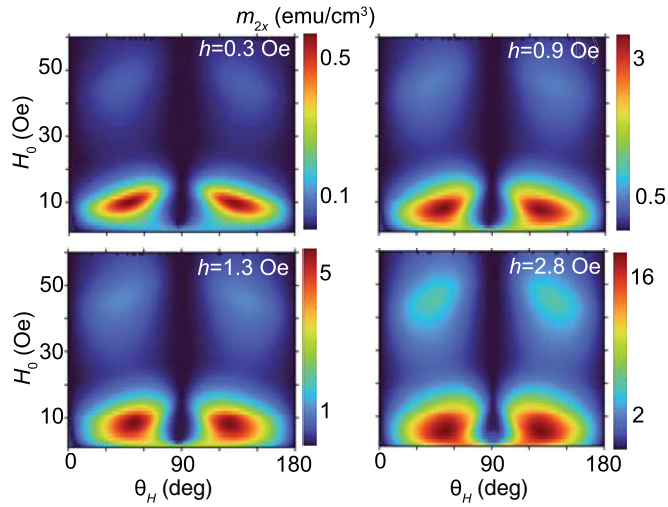

FIG. 3. The experimental dependencies of the second-order magnetization m_{2x} (at 2 GHz) on the strength H_0 and direction θ_H of the static field, obtained for four values of the microwave field h. The frequency of the input signal was 1 GHz.

which reflects the fact that LF and HF peaks grow with h at different rates.

Figure 4(a) shows the profiles of the dependence of the second-order magnetization m_{2x} on H_0 measured at various values of h, and Fig. 4(b) shows the entire map $m_{2x}(H_0, h)$. Note that in these plots, each m_{2x} value was picked for an optimal angle θ_H, at which for a given value of H_0 and h the amplitude m_{2x} is maximum. An interesting feature that can be observed here is that as the amplitude of m_{2x} steadily increases with h, the behaviors of the LF and HF peaks regarding their static field positions differ noticeably. While the field position of the HF peak stays essentially the same for the whole microwave field range (Fig. 4, triangle symbols), the field H_0 of the LF peak gradually decreases with h (Fig. 4, square symbols).

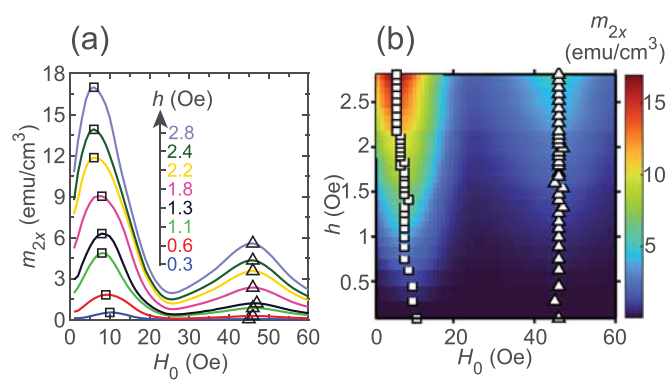

FIG. 4. (a) Second-order magnetization m_{2x} (at 2 GHz) profiles measured as a function of the static field H_0 for several values of the microwave field amplitude h. (b) The map of the $m_{2x}(H_0, h)$ dependence. In both plots, each m_{2x} value was picked for an optimal angle θ_H, at which for a given value of H_0 and h the amplitude m_{2x} is maximum. The square and triangle symbols indicate the low-field (LF) and high-field (HF) peaks, respectively. The frequency of the input signal was 1 GHz.

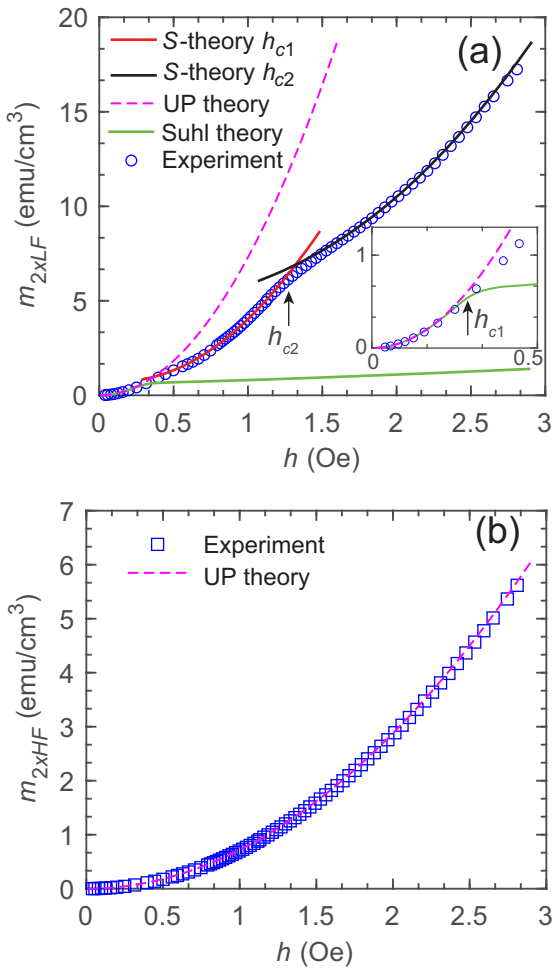

FIG. 5. Second-order magnetization (at 2 GHz) for the low-field (LF) peak $m_{2x\mathrm{LF}}$ (a) and the high-field (HF) peak $m_{2x\mathrm{HF}}$ (b) versus microwave driving field amplitude h. The inset in (a) shows the magnified part of the $m_{2x\mathrm{LF}}(h)$ dependence for the range of $h = 0$–0.5 Oe. The frequency of the input signal was 1 GHz.

Figure 5 shows the experimental dependencies of the second-order magnetization for LF peak $m_{2x\mathrm{LF}}$ [Fig. 5(a)] and HF peak $m_{2x\mathrm{HF}}$ [Fig. 5(b)] on the driving field amplitude h, obtained for the optimal parameters (H_0, θ_H) of the static field. As Fig. 5(b) indicates, the HF peak grows quadratically with h in the whole considered range. In contrast, the LF peak depends quadratically on h only at the very beginning of the dependence $m_{2x\mathrm{LF}}(h)$ [see inset in Fig. 5(a)]. Above a certain *threshold* amplitude of the microwave field $h_{c1} \approx 0.3$ Oe, the $m_{2x\mathrm{LF}}(h)$ dependence starts to deviate from the quadratic one—now $m_{2x\mathrm{LF}}$ increases with h more slowly. Moreover, one can clearly see in Fig. 5(a) that there is a second threshold field $h_{c2} \approx 1.2$ Oe, above which the growth of $m_{2x\mathrm{LF}}$ with h becomes even slower.

This behavior of the LF peak contradicts the predictions of a low-power uniform magnetization precession (UP) theory considered above, according to which both LF and HF peaks should be quadratic in h. This can be seen in Figs. 5(a) and 5(b), where dashed lines show the dependencies calculated using Eq. (6). While for the HF peak [Fig. 5(b)] the uniform precession theory demonstrates excellent agreement with the experiment, the theoretical LF peak increases with h overly optimistically [Fig. 5(a)]. What we observe here for the LF peak is the manifestation of the spin wave instability processes. The question of why this is not the case for the HF peak will be discussed later in this paper. As mentioned in the Introduction, the theory of high-power FMR was first developed by Suhl in the 1950s [5–7]. In the following, we briefly underline its main conclusions, which will help in understanding our experimental results.

B. Suhl spin wave instability processes

The problem of high-power FMR in ferrites was theoretically analyzed by Suhl by first expanding the magnetization vector into a spatial Fourier series, which represents spin waves having amplitudes of m_k. This expansion was then substituted in the LLG equation, where the first-order (in m_k) terms were retained, as well as higher-order terms that contained the products of m_k and the uniform magnetization precession first-order amplitude m_1. The solution showed an interesting result: There are pairs of spin waves with equal and opposite wave vectors $\mathbf{k}$ and $-\mathbf{k}$ that are coupled together by the uniform precession mode. By analogy with a harmonic oscillator, the uniform precession can be considered as a time-dependent parameter that couples two oscillators. This can result in energy transfer through the time-dependent parameter to the oscillators (known as a parametric instability process), which is most efficient when

$$n\omega = \omega_k + \omega_{-k} = 2\omega_k, \tag{7}$$

where ω is the frequency of the driving field, $\omega_k = \omega_{-k}$ are the frequencies of a coupled pair of spin waves, and n is the order of the parametric instability process.

The Suhl spin wave instability theory leads to the following expression for the amplitude m_k [10],

$$m_k(t) = m_{k0} \exp\left(\left[-\eta_k + \sqrt{\left|G_k^{(n)}\right|^2 - (\omega_k - n\omega/2)^2}\right]t\right), \tag{8}$$

where m_{k0} is an initial (thermal level) amplitude, and η_k is the spin wave relaxation rate. The complex coupling coefficient $G_k^{(n)}$, for $n = 2$, which is relevant for our case of second-order instability process (as will be dicussed later), is expressed as [11] $G_k^{(2)} = W_k[(\gamma h)^2/8\omega]$. The coefficient W_k characterizes the coupling between the uniform precession mode and a pair of spin waves. It depends on the magnetic parameters of the sample, H_0, and spin wave parameters: the angle of the in-plane propagation direction θ_k (with respect to $\mathbf{M}_0$) and wave number k.

In essence, Eq. (8) shows that the m_k behavior is governed by the energy balance: When energy pumped from the uniform precession mode to the spin waves during the oscillation period surpasses their energy loss, the m_k amplitudes will grow exponentially in time. This reflects the threshold nature of the parametric instability process, which will onset only when the amplitude of the driving field exceeds a certain threshold value. At this point, the uniform magnetization precession starts losing its energy by transferring it to the spin waves (the driving power being unchanged), resulting in the

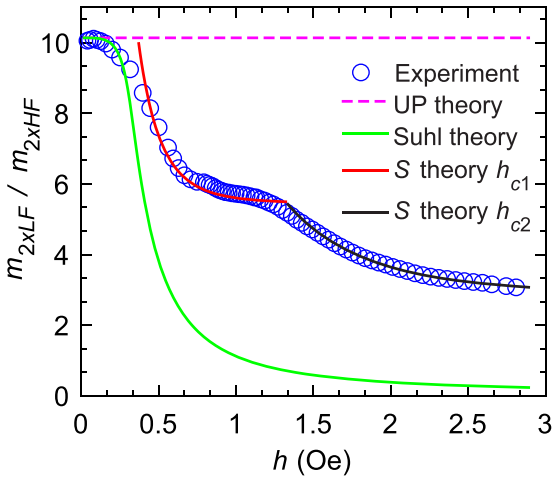

FIG. 6. The ratio of the second-order magnetizations (at 2 GHz) of the low-field (LF) and high-field (HF) peaks versus driving microwave field amplitude h. The frequency of the input signal was 1 GHz.

decrease of the amplitude m_1 and, considering Eqs. (4) and (5), in the decrease of the second harmonic generation as well. This explains the deviation of the experimental dependence $m_{2x\mathrm{LF}}(h)$ from the quadratic law above the driving field amplitude $h_{c1} \approx 0.3$ Oe. Here, energy is going to the parametrically excited spin waves leading to the increase of the effective damping for the uniform precession mode.

The threshold character of the LF peak behavior is more clearly seen in Fig. 6, where the second-order magnetizations ratio $m_{2x\mathrm{LF}}(h)/m_{2x\mathrm{HF}}(h)$ is displayed. In fact, this graph shows the deviation of the LF peak dependence on h from the quadratic law but, being represented in this form, it allows for the direct comparison between theory and experiment. One can see that below the threshold h_{c1}, the ratio has an almost constant value of about 10, in close agreement with the uniform precession theory. However, when h exceeds h_{c1}, the ratio rapidly but nonmonotonically falls off to the value of 3.1 at a maximum driving field of $h = 2.8$ Oe.

From Eq. (8), it is possible to calculate the threshold field h_{c1}. This value is obtained as the minimum threshold among all available spin wave modes (ω_k, θ_k) for considered conditions. For a thin magnetic film, it was shown that the minimum is achieved when $\omega = \omega_k$ and $\theta_k = 0°$ [11]. Thus, the expression for h_{c1} has a form [12]

$$h_{c1} = \Delta H \sqrt{\frac{\Delta H_k}{W_k 4\pi M_s}}, \tag{9}$$

where $\Delta H_k = 2\eta_k/\gamma$. For a thin permalloy film, ΔH_k is usually $\approx 0.5\Delta H$ [11], and the W_k coefficient (at 1 GHz) is about 0.12 [12]. For the parameters ΔH and M_s of our sample, Eq. (9) yields a threshold field of 0.38 Oe, which is close to the experimental value $h_{c1} \approx 0.3$ Oe of the LF peak. At this threshold value of the microwave field (0.3 Oe), the amplitude of the first-order component $m_{1\theta}$ [obtained from the $m_{2x\mathrm{LF}}$ using Eq. (4)] is 59 emu/cm^3, and the corresponding uniform magnetization precession angle $\theta_{Mc} \approx \arcsin(m_{1\theta}/M_s)$ is 3.9°. We note that this value of the precession angle at the threshold agrees well with the experimental data obtained by other authors for thin permalloy films [11,15].

According to the Suhl parametric instability theory, when the microwave field exceeds the threshold h_{c1}, the growth of the uniform precession angle with h ceases—there is a lockup of the precession cone angle at its threshold value θ_{Mc}. The lockup occurs due to a back reaction effect. Above the threshold, the parametrically excited spin waves are pumping energy out of the uniform precession mode. Because in the Suhl theory, the exponential growth of m_k amplitudes is not limited, the energy transfer will continue until the uniform precession angle drops below the threshold. Then the parametric process stops, and the uniform magnetization precession can grow again. This can be imagined as a transient process that, due to the damping in the system, is stabilized to a steady state with the precession angle just below the threshold level. From this follows that the effective "nonlinear" microwave susceptibility χ_n should rapidly decrease with h at FMR. Taking into account two-magnon scattering effects that occur at FMR, Suhl obtained the following expression for the imaginary part of the resonance susceptibility χ_n [7],

$$\frac{\chi''_n}{\chi''} = \frac{A_n + 1}{A_n + [1 - (\chi''_n/\chi'')^4 (h/h_{c1})^4]^{-1/2}}, \tag{10}$$

where χ'' is an imaginary part of the linear susceptibility at FMR, defined by Eq. (2), and A_n is a parameter that is inversely proportional to the relative contribution of scattering effects to the total FMR linewidth.

Based on Eqs. (10) and (4), we have calculated the LF peak second-order magnetization $m_{2x\mathrm{LF}}$ as a function of the microwave field h and the ratio $m_{2x\mathrm{LF}}/m_{2x\mathrm{HF}}$ for the best-fit value of $A_n = 10$. The results are presented in Figs. 5(a) and 6 by the green lines. As one can see, the Suhl theory agrees with the experimental results only near the threshold. Above it, the calculated $m_{2x\mathrm{LF}}$ is almost constant, which results in a sharp decrease in the $m_{2x\mathrm{LF}}/m_{2x\mathrm{HF}}$ ratio. This contradicts remarkably the experimental behavior of $m_{2x\mathrm{LF}}$, which, albeit slower, keeps growing steadily with h above the threshold. Note also that in the experiment, there is no visible lockup at all. This discrepancy indicates that for an adequate description of the high-power FMR experiments well above the threshold in permalloy films, it is necessary to consider other mechanisms that limit the growth of parametric spin waves.

C. Phase limiting mechanism

Zakharov, L'vov, and Starobinets, in the framework of their S theory, showed [22,30] that there is an additional, dephasing, effect that limits the exponential growth of parametric spin wave amplitudes. In the solution of the equation of motion, the authors considered high-order terms containing $m_k m_{k1}$ products, which describe the interactions between pairs of parametric spin waves. The analysis revealed that because of these four-wave interactions, as the m_k amplitudes increase, the phase between the uniform magnetization precession mode and a pair of spin waves deviates from its optimal value. This results in a decrease of the energy flow from the uniform precession mode and saturation (in time dependence) of the m_k amplitudes at some finite level. Because of this nonlinear limiting mechanism, the uniform precession

amplitude can still grow with h above the threshold. Based on the S theory, L'vov derived an equation that describes the behavior of the reduced amplitude of the uniform magnetization precession at FMR [22], where the phase limiting mechanism was taken into account. Considering Eq. (4), for the second-order magnetization component $m_{2x\mathrm{LF}}$ this equation can be written as

$$r\frac{m_{2x\mathrm{LF}}}{m^c_{2x\mathrm{LF}}}+\sqrt{\left(\frac{m_{2x\mathrm{LF}}}{m^c_{2x\mathrm{LF}}}\right)^2-1}=r\frac{h}{h_c}\sqrt{\frac{m_{2x\mathrm{LF}}}{m^c_{2x\mathrm{LF}}}}, \qquad (11)$$

where $m^c_{2x\mathrm{LF}}$ and h_c are the threshold values of the second-order magnetization and the microwave field, respectively. The coefficient r is proportional to W_{kk1}/W_k, where W_{kk1} is a coupling coefficient for parametric spin waves. That is, in Eq. (11), r characterizes the relative impact of spin wave interactions on the uniform magnetization precession dynamics. For example, when there are no spin-wave–spin-wave interactions, $r = 0$, and $m_{2x\mathrm{LF}} = m^c_{2x\mathrm{LF}}$, which corresponds to the lockup of the Suhl instability theory. And conversely, at large $r \gg 1$, $m_{2x\mathrm{LF}} \sim h^2$ meaning that the spin wave coupling is so high it completely prevents the energy transfer from the uniform precession mode, and it behaves like there are no parametric processes at all. This reflects the fact that the uniform precession theory and the Suhl theory represent two extreme cases, in one of which the magnetization dynamics is not affected by the spin waves at all and in the other, all the energy of uniform precession above the threshold goes to the parametric spin waves. However, the experimental data show some intermediate results, and according to the S theory, the r coefficient value should be of the order of unity.

Using Eq. (11), we have calculated the theoretical dependence of $m_{2x\mathrm{LF}}(h)$ for the experimental values of the first threshold, $h_c = h_{c1} = 0.3$ Oe, $m^c_{2x\mathrm{LF}} = 0.5\,\mathrm{emu/cm^3}$, and the best-fit value of $r = 0.45$. As one can see in Figs. 5(a) and 6, for the microwave field ranging between the first and second thresholds, there is excellent agreement between the $m_{2x\mathrm{LF}}(h)$ dependence based on the S theory (solid red line) and the experimental data. Note also that the value of the coefficient $r = 0.45$ is quite close to the values obtained by other authors in the same kind of analysis, 0.6 in Ref. [12] and 0.63 in Ref. [15].

One of the consequences of the dephasing effect is that another group of spin waves can be parametrically excited in the sample. Recall that the threshold field was obtained from Eq. (8) as a minimum among all available spin wave modes. As was mentioned previously, above the threshold, the amplitudes of the first pair of spin waves are limited, and the uniform magnetization precession amplitude continues to increase with h. At some point, the uniform precession amplitude will be high enough to overcome the energy loss of another spin wave mode with a higher threshold, which results in its parametric excitation and a subsequent additional increase of the effective damping for the uniform precession mode. The spin-wave–spin-wave interaction plays an important role in this process, as it prevents the earlier onset of parametric spin waves with $\theta_k \neq 0^\circ$. This "stage by stage" excitation of parametric spin waves was first predicted in the framework of the S theory and then experimentally confirmed for ferrites in the case of parallel pumping [30,31]. Our experimental data can be understood in terms of the stage by stage process too. The distinctive change in the $m_{2x\mathrm{LF}}(h)$ dependence at $h_{c2} \approx 1.2$ Oe can be interpreted as the excitation of the second pair of parametric spin waves at the second threshold field h_{c2}. This explains why the first curve based on Eq. (11) and h_{c1} value fits the experimental data only between h_{c1} and h_{c2}: The spin waves excited at the second threshold slow down further the growth of $m_{2x\mathrm{LF}}$.

Using Eq. (11), we have calculated the $m_{2x\mathrm{LF}}(h)$ dependence above the second threshold, shown by the solid black lines in Figs. 5(a) and 6. Note, however, that because this equation was derived specifically for the first threshold case, it can be used only for a qualitative analysis of the $m_{2x\mathrm{LF}}$ response above h_{c2}. We obtained the best fit to the experiment for almost the same value of the coefficient $r = 0.42$, but for the threshold field $h_{c2} = 1$ Oe ($m^c_{2x\mathrm{LF}} = 3.8\,\mathrm{emu/cm^3}$), which is a bit lower than that determined from the data ($\approx$1.2 Oe). Nevertheless, the character of the calculated dependence agrees well with the measurements, indicating that the same type of processes governed by the phase limiting mechanism occur above the second threshold.

We would like to emphasize the advantage of using, in our measurements, the microwave driving field with a relatively low frequency of $f = 1$ GHz. As follows from Eq. (9), the threshold field h_{c1} is proportional to f. Although the maximum microwave field amplitude was a moderate 2.8 Oe, in relative units h/h_{c1} (so-called "supercriticality"), we have reached a value of about 10, which allowed us to detect the second threshold at $h/h_{c1} = 4$. For example, in experiments with permalloy films performed at 9.11 GHz, the threshold field at FMR was 2.7 Oe [11]. Therefore, although the maximum pumping field was quite high, about 10 Oe, in the units h/h_{c1} it was only 3.7.

Note that the same experimental measurements and theoretical analysis, as presented above in Secs. III and IV, were also performed for another sample, a 100 nm thick $Ni_{70}Fe_{30}$ film. The data for this sample are given in the Supplemental Material [25]. In general, the results obtained for this sample are similar to the data just presented, where the differences are mainly caused by the differences in the magnetic parameters, in particular, higher M_s, H_u, and damping α. For the $Ni_{70}Fe_{30}$ film, both the first and second microwave field thresholds are also observed ($h_{c1}\approx 0.2$ Oe, $h_{c2} \approx 0.8$ Oe), and Eq. (11) fits fairly well the $m_{2x\mathrm{LF}}(h)$ dependence as well, for almost the same values of the coefficient r.

D. Difference in the power-dependent behavior of the LF and HF peaks

In this last section, we return to the question of why there is a difference in the power-dependent behavior for the LF and HF peaks. The spin wave instability processes can occur only in conditions that allow for the excitation of spin waves. These conditions are determined by the spin wave dispersion relation, which for a thin magnetic film with uniaxial anisotropy

has the following form [32]:

$$\begin{aligned}\omega_k &= \sqrt{\omega_{ky}\omega_{k\theta}},\\ \omega_{ky} &= \gamma[H_0\cos(\theta_H-\theta_M)+H_u\cos^2\theta_M+Dk^2+4\pi M_s N_k],\\ \omega_{k\theta} &= \gamma[H_0\cos(\theta_H-\theta_M)+H_u\cos 2\theta_M+Dk^2+4\pi M_s\sin^2\theta_k(1-N_k)].\end{aligned} \tag{12}$$

Here $N_k = (1-e^{-kd})/kd$ is the demagnetization factor, with d being the thickness of the film, and $D = 2A/M_s$, where A is the exchange stiffness constant, with the typical value for permalloy of 1×10^{-6} erg/cm.

Figure 7 shows the dependence of $f_k = \omega_k/2\pi$ on k calculated with Eq. (12) for $\theta_k = 0^\circ$, and the experimental parameters of the $Ni_{80}Fe_{20}$ sample. In the graph, two lines are drawn: The solid blue one is for the static field $H_0 = 10.6$ Oe and $\theta_H = 45^\circ$, which corresponds to the LF peak, and the dashed red one is for $H_0 = 46.5$ Oe and $\theta_H = 43^\circ$, corresponding to the HF peak. These lines represent boundaries below which, for a given value of H_0, spin waves cannot propagate. The field H_0 of the LF peak corresponds to the FMR at a driving frequency of $f_1 = 1$ GHz. The frequencies of the spin waves in the conditions of the LF peak can only be almost equal or higher than f_1. Considering the energy transfer condition (7), we can see that in a thin magnetic film, the lowest order of parametric instability process at FMR is $n = 2$. However, for the field $H_0 = 46.5$ Oe of the HF peak, the spin wave spectrum is located far above the f_1 frequency rendering the second-order parametric process impossible to occur in this case. In fact, the lowest for these conditions is the fourth-order process, with a much higher threshold value of microwave field.

In practice, the HF peak can serve as a reference signal in high-power experiments. The agreement of its behavior with the uniform magnetization precession theory will indicate that (1) the measurement setup is well calibrated, and (2) the magnetization dynamics is not affected by other factors, for example, heating. Therefore, while this is the case, the peculiarities observed in the LF peak dependencies (that are measured almost simultaneously with the HF one) are most probably caused by the spin wave instability processes.

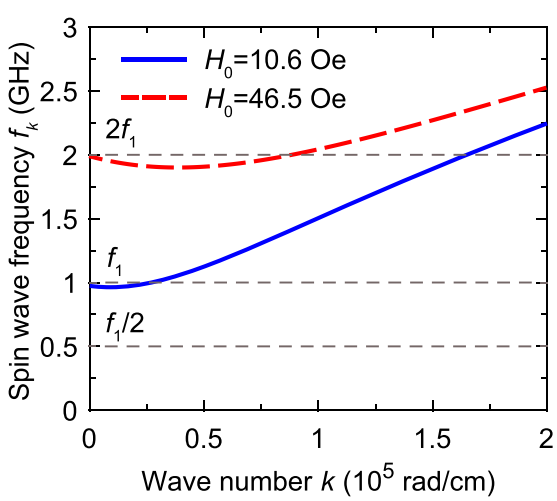

FIG. 7. Spin wave dispersion relation of a thin magnetic film calculated for two values of the static field H_0 corresponding to the low-field and high-field peaks. $f_1 = 1$ GHz is the frequency of the experimental driving field.

In this context, let us return to Fig. 4, which shows that the LF peak field position gradually decreases from $H_0 = 11$ Oe at $h = 0.09$ Oe to $H_0 = 6$ Oe at $h = 2.8$ Oe, corresponding to the FMR frequency positive shift of 300 MHz. This is counterintuitive as, based on the classic FMR theory, one would expect that as the magnetization precession cone expands, the FMR frequency decreases [1]. The increase of the FMR frequency with power (or decrease of the FMR field) was observed in previous works [11,14,16] and was associated with the nonlinear interaction of spin waves [14,33]. These spin waves can be excited both through the parametric processes discussed above and also due to the two-magnon scattering. Comparing the second-order magnetizations of the LF and HF peaks' dependencies on h (Fig. 5), we can see that at $h = 2.8$ Oe, $m_{2x\mathrm{HF}} = 5.6$ emu/cm^3, and its field position has not changed. At the same time, the LF peak reaches this value $m_{2x\mathrm{LF}} = 5.6$ emu/cm^3 at $h = 1.2$ Oe, but at this point, its field position is decreased by 3 Oe with respect to the initial (at $h = 0.09$ Oe) value. Therefore, for the same magnetization precession angles, in one case (where spin wave modes are available), there is a shift, and in the other (where the spin wave spectrum is above the driving frequency), there is not. This fact is experimental evidence showing that the nonlinear FMR frequency/field shift is indeed caused by the excited spin waves.

V. CONCLUSIONS

In this paper, we have investigated second harmonic generation in a thin permalloy film at low- and high-power levels of microwave signals, at a frequency of 1 GHz. It has been shown that the output signal at twice the frequency of the driving field was formed by two second-order dynamic components of the uniform magnetization—the longitudinal one, which has a maximum at a low static magnetic field (LF peak, coincides with FMR field), and the transverse one, with a maximum at the much higher field (HF peak). The experimental dependence of the LF peak on the microwave field amplitude clearly revealed the onset of the Suhl second-order spin wave instability processes. The complicated nonlinear behavior observed for the LF peak above the threshold field (≈0.3 Oe) has been explained through the phase limiting mechanism following the S theory of Zakharov, L'vov, and Starobinets. The use of a driving field with a relatively low frequency allowed us to observe in thin metallic films for the LF peak the additional (second) threshold, at a moderate microwave field amplitude (≈1.2 Oe). This second threshold was interpreted as the evidence of the excitation of another group of parametric spin waves, again in accordance with the

predictions of the *S* theory. The apparent immunity of the HF peak to the parametric processes was explained simply by the fact that at the conditions of its appearance, the spin wave band shifted far above the driving frequency of 1 GHz, to the region where the occurrence of low-order instability processes is prohibited. This feature of the HF peak can be used in practice in high-power FMR experiments for the separation of the effects in the uniform mode behavior caused by the spin waves, in particular, parametrically excited, as was illustrated by considering the power-dependent FMR field negative shift. The obtained results demonstrate that the dephasing effects caused by the interactions between pairs of parametric spin waves play a crucial role in the above-threshold response of thin magnetic films at FMR, and the measurement of the second harmonic generation is an effective approach for the study of such effects in magnetization dynamics of thin-film magnetic samples.

ACKNOWLEDGMENTS

This work was supported by the Russian Science Foundation under Grant No. 19-72-10047. The equipment of the Krasnoyarsk Regional Center of Research Equipment of Federal Research Center "Krasnoyarsk Science Center SB RAS" was used during the measurements.

[1] A. G. Gurevich and G. A. Melkov, *Magnetization Oscillations and Waves* (CRC Press, Boca Raton, FL, 1996).
[2] P. E. Wigen, *Nonlinear Phenomena and Chaos in Magnetic Materials* (World Scientific, Singapore, 1994).
[3] K. Livesey, Nonlinear behavior in metallic thin films and nanostructures, in *Handbook of Surface Science*, Vol. 5 (Elsevier, Amsterdam, 2015), pp. 169–214.
[4] N. Bloembergen and S. Wang, Relaxation effects in para- and ferromagnetic resonance, Phys. Rev. **93**, 72 (1954).
[5] H. Suhl, The nonlinear behavior of ferrites at high microwave signal levels, Proc. IRE **44**, 1270 (1956).
[6] H. Suhl, The theory of ferromagnetic resonance at high signal powers, J. Phys. Chem. Solids **1**, 209 (1957).
[7] H. Suhl, Note on the saturation of the main resonance in ferromagnetics, J. Appl. Phys. **30**, 1961 (1959).
[8] E. Schlömann, J. J. Green, and U. Milano, Recent developments in ferromagnetic resonance at high power levels, J. Appl. Phys. **31**, S386 (1960).
[9] J. D. Adam, Mitigate the interference: Nonlinear frequency selective ferrite devices, IEEE Microwave Mag. **15**, 45 (2014).
[10] S. Y. An, P. Krivosik, M. A. Kraemer, H. M. Olson, A. V. Nazarov, and C. E. Patton, High power ferromagnetic resonance and spin wave instability processes in permalloy thin films, J. Appl. Phys. **96**, 1572 (2004).
[11] H. M. Olson, P. Krivosik, K. Srinivasan, and C. E. Patton, Ferromagnetic resonance saturation and second order Suhl spin wave instability processes in thin permalloy films, J. Appl. Phys. **102**, 023904 (2007).
[12] T. Gerrits, P. Krivosik, M. L. Schneider, C. E. Patton, and T. J. Silva, Direct Detection of Nonlinear Ferromagnetic Resonance in Thin Films by the Magneto-Optical Kerr Effect, Phys. Rev. Lett. **98**, 207602 (2007).
[13] B. K. Kuanr, Y. V. Khivintsev, A. Hutchison, R. E. Camley, and Z. J. Celinski, Nonlinear microwave effects on iron based microstrip filter, IEEE Trans. Magn. **43**, 2645 (2007).
[14] Y. Khivintsev, B. Kuanr, T. J. Fal, M. Haftel, R. E. Camley, Z. Celinski, and D. L. Mills, Nonlinear ferromagnetic resonance in permalloy films: A nonmonotonic power-dependent frequency shift, Phys. Rev. B **81**, 054436 (2010).
[15] C. Bi, X. Fan, L. Pan, X. Kou, J. Wu, Q. Yang, H. Zhang, and J. Q. Xiao, Electrical detection of nonlinear ferromagnetic resonance in single elliptical permalloy thin film using a magnetic tunnel junction, Appl. Phys. Lett. **99**, 232506 (2011).
[16] H. G. Bauer, P. Majchrak, T. Kachel, C. H. Back, and G. Woltersdorf, Nonlinear spin-wave excitations at low magnetic bias fields, Nat. Commun. **6**, 8274 (2015).
[17] Th. Gerrits, M. Schneider, A. Kos, and T. Silva, Large-angle magnetization dynamics measured by time-resolved ferromagnetic resonance, Phys. Rev. B **73**, 094454 (2006).
[18] V. E. Demidov, S. Urazhdin, H. Ulrichs, V. Tiberkevich, A. Slavin, D. Baither, G. Schmitz, and S. O. Demokritov, Magnetic nano-oscillator driven by pure spin current, Nat. Mater. **11**, 1028 (2012).
[19] G. A. Melkov, Y. V. Koblyanskiy, R. A. Slipets, A. V. Talalaevskij, and A. N. Slavin, Nonlinear interactions of spin waves with parametric pumping in permalloy metal films, Phys. Rev. B **79**, 134411 (2009).
[20] T. Brächer, P. Pirro, and B. Hillebrands, Parallel pumping for magnon spintronics: Amplification and manipulation of magnon spin currents on the micron-scale, Phys. Rep. **699**, 1 (2017).
[21] J. L. Melchor, W. P. Ayres, and P. H. Vartanian, Microwave frequency doubling from 9 to 18 KMC in ferrites, Proc. IRE **45**, 643 (1957).
[22] V. S. L'vov, *Wave Turbulence under Parametric Excitation* (Springer-Verlag, Berlin, 1994).
[23] B. A. Belyaev, A. V. Izotov, and A. A. Leksikov, Magnetic imaging in thin magnetic films by local spectrometer of ferromagnetic resonance, IEEE Sens. J. **5**, 260 (2005).
[24] B. A. Belyaev, A. V. Izotov, P. N. Solovev, and I. A. Yakovlev, Determination of magnetic anisotropies and miscut angles in epitaxial thin films on vicinal (111) substrate by the ferromagnetic resonance, J. Magn. Magn. Mater. **440**, 181 (2017).
[25] See Supplemental Material at http://link.aps.org/supplemental/10.1103/PhysRevB.106.064406 for distributions of magnetic parameters across the films' surfaces, and results for the $Ni_{70}Fe_{30}$ film.
[26] B. A. Belyaev, A. O. Afonin, A. V. Ugrymov, I. V. Govorun, P. N. Solovev, and A. A. Leksikov, Microstrip resonator for nonlinearity investigation of thin magnetic films and magnetic frequency doubler, Rev. Sci. Instrum. **91**, 114705 (2020).
[27] A. A. Leksikov, A. M. Serzhantov, I. V. Govorun, A. O. Afonin, A. V. Ugryumov, and A. A. Leksikov, Microstrip diplexer with π-shaped matching circuit, Prog. Electromagn. Res. Lett. **88**, 59 (2020).

[28] T. J. Silva, C. S. Lee, T. M. Crawford, and C. T. Rogers, Inductive measurement of ultrafast magnetization dynamics in thin-film permalloy, J. Appl. Phys. **85**, 7849 (1999).

[29] P. N. Solovev, A. O. Afonin, B. A. Belyaev, N. M. Boev, I. V. Govorun, A. V. Izotov, A. V. Ugrymov, and A. A. Leksikov, Second harmonic generation in thin permalloy film, J. Phys. Appl. Phys. **54**, 425002 (2021).

[30] V. E. Zakharov, V. S. L'vov, and S. S. Starobinets, Spin-wave turbulence beyond the parametric excitation threshold, Sov. Phys. Usp. **17**, 896 (1975).

[31] V. V. Zaushkin, V. S. L'vov, S. L. Musher, and S. S. Starobinets, Proof of stage-by-stage excitation of parametric spin waves, Zh. Eksp. Teor. Fiz. Pis'ma Red. **14**, 310 (1971).

[32] R. Arias and D. L. Mills, Extrinsic contributions to the ferromagnetic resonance response of ultrathin films, Phys. Rev. B **60**, 7395 (1999).

[33] P. Krivosik, K. Srinivasan, H. M. Olson, and C. E. Patton, High power ferromagnetic resonance in thin permalloy films—the steady state response, threshold modifications, and magnon scattering, in *INTERMAG 2006—IEEE International Magnetics Conference, San Diego, CA* (IEEE, New York, 2006), p. 70.